JOC Article

On the Mechanism of the Palladium Catalyzed Intramolecular Pauson−Khand-Type Reaction

Yu Lan,[†] Lujiang Deng,[†] Jing Liu,[†] Can Wang,[†] Olaf Wiest,*[,‡] Zhen Yang,*[,†] and Yun-Dong Wu*[,†,§]

College of Chemistry, Peking University, Beijing, 100871, China, Department of Chemistry, The Hong Kong University of Science and Technology, Clear Water Bay, Kowloon, Hong Kong, China, and Department of Chemistry and Biochemistry, University of Notre Dame, Notre Dame, Indiana 46556

chydwu@ust.hk; zyang@pku.edu.cn; owiest@nd.edu

Received May 3, 2009

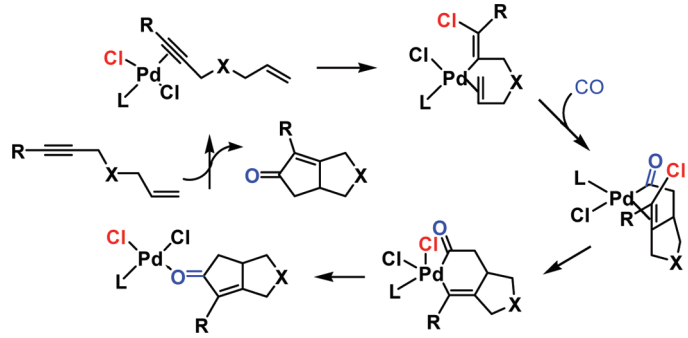

Density functional theory calculations and experimental studies have been carried out on the intramolecular Pauson−Khand-Type reaction mediated by a $PdCl_2$-thiourea catalyst, which proceeds under mild reaction conditions and provides a useful alternative to traditional Pauson−Khand reactions. The classical mechanism of the Pauson−Khand reaction involving the alkyne/alkene C−C bond formation as the key step has been found to be energetically unfavorable and is not in line with the experimental observations. A novel reaction mechanism has been proposed for the reaction. The first step involves the *cis*-halometalation of the alkyne, followed by sequential alkene and carbonyl insertion. The rate-determining fourth step is an intramolecular C−Cl oxidative addition, leading to a Pd^{IV} intermediate. A C−C bond formation by reductive elimination completes the reaction. The mechanism is in agreement with the key experimental observations including (1) the need of a chloride for catalytic activity and the absence of catalysis with $Pd(OAc)_2$ alone; (2) the rate acceleration by the addition of LiCl; both with $PdCl_2$ and $Pd(OAc)_2$ catalysts; and (3) the preferred formation of the *trans* diastereomer in substituted cases. The *cis* halometalation and the formation and stability of the Pd^{IV} intermediate is studied in detail and provides general insights into these novel steps.

Introduction

The Pauson−Khand reaction (PKR) is formally a [2 + 2 + 1] cycloaddition in which an alkyne, an alkene and a carbon monoxide couple to form a cyclopentenone.[1] The PKR is widely used for the effective synthesis of cyclopentenone frameworks,[2] many of which appear in natural products.[3] Although the

[†] Peking University.
[‡] University of Notre Dame.
[§] The Hong Kong University of Science and Technology.

(1) (a) Khand, I. U.; Knox, G. R.; Pauson, P. L.; Watts, W. E. *J. Chem. Soc., Chem. Commun.* **1997**, 36. (b) Khand, I. U.; Knox, G. R.; Pauson, P. L.; Watts, W. E.; Foreman, M. I. *J. Chem. Soc., Perkin Trans. 1* **1973**, 975. (c) Khand, I. U.; Knox, G. R.; Pauson, P. L.; Watts, W. E.; Foreman, M. I. *J. Chem. Soc., Perkin Trans. 1* **1973**, 977.

(2) (a) Shibata, T. *Adv. Synth. Catal.* **2006**, *348*, 2328. (b) Gibson, S. E.; Mainolfi, N. *Angew. Chem., Int. Ed.* **2005**, *44*, 3022. (c) Jaime, B. U.; Loreto, A.; Leticia, P. S.; Gema, D.; Javier, P. C. *Chem. Soc. Rev.* **2004**, *33*, 32. (d) Pauson, P. L. In *Organometallics in Organic Synthesis. Aspects of a Modern Interdisciplinary Field*; de Meijere, A., tom Dieck, H., Eds.; Springer: Berlin, 1988; p 233.

(3) (a) Gao, P.; Xu, P. F.; Zhai, H. *J. Org. Chem.* **2009**, *74*, 2592. (b) Eduardo, A.; Jaime, B. U.; Delbrin, A.; Gema, D.; Javier, P. C. J. *Organometall. Chem.* **2008**, *693*, 2431. (c) Kaneda, K.; Honda, T. *Tetrahedron* **2008**, *64*, 11589. (d) Nadu, C. E.; Lovely, C. J. *Org. Lett.* **2007**, *9*, 4697. (e) Kubota, H.; Lim, J.; Depew, K. M.; Schreiber, S. L. *Chem. Biol.* **2002**, *9*, 265.

10.1021/jo900919v CCC: $40.75
Published on Web 05/26/2009

SCHEME 1. Pd^{II} Catalyzed Pauson−Khand-Type Reaction

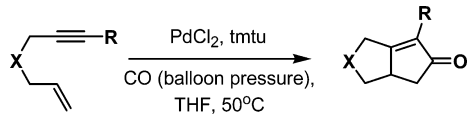

reaction is most commonly catalyzed by Co,[4] the use of several other transition metals such as Ti,[5] Zr,[5b,6] Ni[7], Mo,[8] Ru,[9] Rh,[9d,10] and Ir[11] in Pauson−Khand-like reactions (for convenience it is still referred to as PKR hereafter) has been described. Recently, one of us found that $PdCl_2$ coordinated to a thiourea ligand could also catalyze an intramolecular PKR, as shown in Scheme 1.[12] With reaction temperatures of 50 °C and balloon pressure carbon monoxide, the reaction conditions are very mild. Several interesting features of the novel reaction were observed,[12] namely that; (a) the reaction could be catalyzed by $PdCl_2$ alone, but the yield is low; (b) addition of thiourea, especially tetramethyl thiourea (tmtu) greatly increases the reaction yield; (c) the presence of chloride is essential, and the reaction could not be catalyzed by $Pd(OAc)_2$ or $Pd(dba)_2$; (d) added Lewis acids such as LiCl can increase the reaction rate and ultimately the yield; (e) the stereochemistry of $PdCl_2$ catalyzed PKR is different with other metal-catalyzed PKR in that substituted substrates selectively form the *trans* diastereomer, thus providing access to different stereoisomers. These observations are intriguing and cannot be explained by the widely accepted mechanism of the PKR, but an explanation of the experimental findings is not obvious. We therefore decided to pursue a detailed computational study of the reaction mechanism.

In principle, the palladium catalyzed 1,*n*-enyne cycloisomerization can proceed via two possible pathways shown in Scheme 2.[13] In the first one (pathway A), a palladacyclopentene is formed via an oxidative cyclization. Some 1,*n*-enyne cycloisomerizations where the catalyst is $Pd_2(dba)_3$[14] or palladacyclopentadiene[15] are reported to occur via this route. After the oxidative cyclization, which is thought to be the rate-determining step, CO inserts to the Pd−C bond. After the reductive elimination, cyclopentenone is formed. This pathway is in analogy to the catalytic cycle proposed by Magnus et al.[13] for the $Co_2(CO)_8$ catalyzed PKR[16,17] that forms the basis for the proposed mechanisms of almost all the transition metal-catalyzed PKRs. However, this pathway does not explain the current experimental observations that are described above. Specifically, it does not explain the essential role of the chloride anion, observed stereochemistry, and the acceleration of the reaction by added LiCl.[12]

SCHEME 2. Two Possible Competitive Mechanisms of Palladium Catalyzed 1,6-Enyne PKR

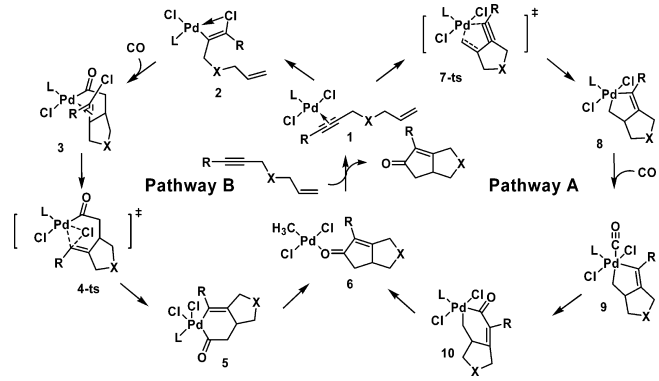

In the alternative pathway B, the reaction is initiated by a *cis*-addition of palladium and chloride to the alkyne in a regioselective fashion where the chloride is transferred to the terminal position of alkyne. This initiation step has been shown to be also possible for the cases of Pd^{II}[18] or hydrogenated Pd^{0}[19] catalyzed cycloisomerizations. After insertions of alkene and CO, Pd is oxidatively inserted into the vinyl-chloride bond, leading to the formation of the same intermediate as in pathway A. In both cases, the cyclopentenone product is formed after the reductive elimination and closing of the catalytic cycle.

Although Pathway B appears reasonable and in agreement with the experimental observations, as will be discussed in more detail below, there is to the best of our knowledge no precedence for such a mechanism. Here, we present a study of the two pathways shown in Scheme 2. Starting from Nakamura's work[16] for the Co-catalyzed PKR, we investigated the cyclizations of 1-allyloxy-2-butyne as a typical *1,6*-enyne by $Pd(Cl)_2$ and tetramethyl thiourea (tmtu) as the ligand to model the Pd-catalyzed PKR. We will start by investigating the energetics

(4) (a) Muller, J. L.; Rickers, A.; Leitner, W. *Adv. Synth. Catal.* **2007**, *349*, 287. (b) Gibson, S. E.; Stevenazzi, A. *Angew. Chem., Int. Ed.* **2003**, *42*, 1800. (c) Fletcher, A. J.; Christie, S. D. R. *J. Chem. Soc., Perkin Trans. 1* **2000**, 1657.

(5) (a) Hicks, F. A.; Kablaoui, N. M.; Buchwald, S. L. *J. Am. Chem. Soc.* **1996**, *118*, 9450; **1994**, *116*, 8593. (b) Hicks, F. A.; Berk, S. C.; Buchwald, S. L. *J. Org. Chem.* **1996**, *61*, 2713. (c) Hicks, F. A.; Buchwald, S. L. *J. Am. Chem. Soc.* **1996**, *118*, 11688. (d) Hicks, F. A.; Buchwald, S. L. *J. Am. Chem. Soc.* **1999**, *121*, 7026. (e) Hicks, F. A.; Kablaoui, N. M.; Buchwald, S. L. *J. Am. Chem. Soc.* **1999**, *121*, 5881. (f) Zhao, Z. B.; Ding, Y.; Zhao, G. *J. Org. Chem.* **1998**, *63*, 9285.

(6) (a) Negishi, E.-I.; Holmes, S. J.; Tour, J. M.; Miller, J. A. *J. Am. Chem. Soc.* **1985**, *107*, 1568. (b) Agnel, G.; Negishi, E.-I. *J. Am. Chem. Soc.* **1991**, *113*, 7424.

(7) (a) Tamao, K.; Kobayashi, K.; Ito, Y. *J. Am. Chem. Soc.* **1988**, *110*, 1286. (b) Zhang, M.; Buchwald, S. L. *J. Org. Chem.* **1996**, *61*, 4498.

(8) (a) Mukai, C.; Uchiyama, M.; Hanaoka, M. *J. Chem. Soc. Chem. Commun.* **1992**, 1014. (b) Jeong, N.; Lee, S. L.; Lee, B. Y.; Chung, Y. K. *Tetrahedron Lett.* **1993**, *34*, 4027. (c) Kent, J. L.; Wan, H. H.; Brummond, K. M. *Tetrahedron Lett.* **1995**, *36*, 2407. (d) Adrio, J.; Rivero, M. R.; Carretero, J. C. *Org. Lett.* **2005**, *7*, 431. (e) Adrio, J.; Carretero, J. C. *J. Am. Chem. Soc.* **2007**, *129*, 778.

(9) (a) Morimoto, T.; Chatani, N.; Fukumoro, Y.; Murai, S. *J. Org. Chem.* **1997**, *62*, 3762. (b) Kondo, T.; Suzuki, N.; Okada, T.; Mitsudo, T. *J. Am. Chem. Soc.* **1997**, *119*, 6187. (c) Koga, Y.; Kobayashi, T.; Narasaka, K. *Chem. Lett.* **1998**, 249. (d) Kobayashi, T.; Koga, Y.; Narasaka, K. *J. Organomet. Chem.* **2001**, *624*, 73. (e) Kondo, T.; Nomura, M.; Ura, Y.; Wada, K.; Mitsudo, T.-A. *J. Am. Chem. Soc.* **2006**, *128*, 14816.

(10) (a) Koga, Y.; Kobayashi, T.; Narasaka, K. *Chem. Lett.* **1998**, 249. (b) Jeong, N.; Lee, S.; Sung, B. K. *Organometallics* **1998**, *17*, 3642. (c) Jeong, N.; Sung, B. K.; Choi, Y. K. *J. Am. Chem. Soc.* **2000**, *122*, 6771. (d) Fan, B. M.; Xie, J. H.; Li, S.; Tu, Y. Q.; Zhou, Q. L. *Adv. Syn. Cat.* **2005**, *347*, 759.

(11) (a) Shibata, T.; Takagi, K. *J. Am. Chem. Soc.* **2000**, *122*, 9852. (b) Shibata, T.; Toshida, N.; Yamazaki, M.; Maekawa, S.; Takagi, K. *Tetrahedron* **2005**, *61*, 9974.

(12) (a) Tang, Y.; Deng, L.; Zhang, Y.; Dong, G.; Chen, J.; Yang, Z. *Org. Lett.* **2005**, *7*, 1657. (b) Deng, L.; Liu, J.; Huang, J.; Hu, Y.; Chen, M.; Lan, Y.; Chen, J.; Lei, A.; Yang, Z. *Synthesis* **2007**, 2565.

(13) (a) Magnus, P.; Príncipce, L. M. *Tetrahedron Lett.* **1985**, *26*, 4851. (b) Gimbert, Y.; Lesage, D.; Milet, A.; Fournier, F.; Greene, A. E.; Tabet, J.-C. *Org. Lett.* **2003**, *5*, 4073.

(14) (a) Trost, B. M.; Romero, D. L.; Rise, F. *J. Am. Chem. Soc.* **1994**, *116*, 4268. (b) Yamamoto, Y.; Nagata, A.; Itoh, K. *Tetrahedron Lett.* **1999**, *40*, 5035.

(15) (a) Trost, B. M.; Tanoury, G. J. *J. Am. Chem. Soc.* **1988**, *110*, 1636. (b) Trost, B. M. *Acc. Chem. Res.* **1990**, *23*, 34. (c) Trost, B. M.; Stephen, A.; Hashmi, K. *J. Am. Chem. Soc.* **1994**, *116*, 2183. (d) Trost, B. M.; Yanai, M.; Hoogsteen, K. *J. Am. Chem. Soc.* **1993**, *115*, 5294.

(16) Yamanaka, M.; Nakamura, E. *J. Am. Chem. Soc.* **2001**, *123*, 1703.

(17) (a) Bruin, T. J. M. de.; Milet, A.; Robert, F.; Gimbert, Y.; Green, A. E. *J. Am. Chem. Soc.* **2001**, *123*, 7184. (b) de Bruin, T. J. M.; Milet, A.; Greene, A. E.; Gimbert, Y. *J. Org. Chem.* **2004**, *69*, 1075. (c) Del Valle, C. P.; Milet, A.; Gimbert, Y.; Greene, A. E. *Angew. Chem., Int. Ed.* **2005**, *44*, 5717.

(18) (a) Ji, J.; Wang, Z.; Lu, X. *Organometallics* **1996**, *15*, 2821. (b) Li, J.; Jiang, H.; Chen, M. *J. Org. Chem.* **2001**, *66*, 3627. (c) Wang, Z.; Zhang, Z.; Lu, X. *Organometallics* **2002**, *19*, 775. (d) Lu, X. *Top. Catal.* **2005**, *35*, 73. (e) Zhu, G.; Zhang, Z. *J. Org. Chem.* **2005**, *70*, 3339.

(19) (a) Yamamoto, Y.; Nagata, A.; Nagata, H.; Ando, Y.; Arikawa, Y.; Tatsumi, K.; Itoh, K. *Chem.−Eur. J.* **2003**, *9*, 2469. (b) Yamamoto, Y.; Kuwabara, S.; Ando, Y.; Nagata, H.; Nishiyama, H.; Itoh, K. *J. Org. Chem.* **2004**, *69*, 6697.

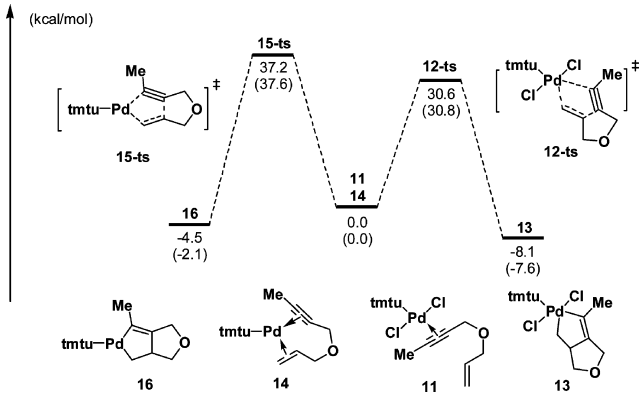

FIGURE 1. Relative Gibbs free energies (in THF) of the initial oxidative coupling step with gas phase Gibbs free energies in parentheses.

and selectivity of the Magnus-type mechanism (pathway A) for the case of the Pd^{II}-tmtu system. We will then study the individual steps of the proposed mechanism (Pathway B). Finally, we will discuss the relationship of the results with the experimental data.

Computational Methods

All calculations were carried out with the GAUSSIAN 03[20] series of programs using the BP86 density functional.[21] Each structure was fully optimized using the SDD basis set for Pd and the 6-31+G(d) basis set for all other atoms. Harmonic frequency calculations were performed for all structures to confirm them as a local minima or transition structures and to derive the thermochemical corrections for the enthalpies and free energies. Solvent effects were evaluated using the Polarizable Continuum Model (PCM)[22] using simple united atom topological model radii with the default parameters for THF. All enthalpies and the Gibbs free energies in the text are in kcal/mol and are calculated for standard conditions (298 K, atm) and are corrected for solvation effects as described above. All distances are given in Å.

Results and Discussion

C−C Coupling Pathway. Earlier experimental and computational studies of the Magnus mechanism for the PKR identified the oxidative addition as the rate determining step of the reaction.[16,17] We therefore started the investigation by calculating the free energies of activation for the enyne oxidative coupling step. Both Pd(0) to Pd(II) and Pd(II) to Pd(IV) mechanism were studied. The results for this mechanism are summarized in Figure 1. Only the alkyne part of enyne is coordinated to $PdCl_2$-tmtu to form the intermediate **11**. The pentacoordinated species where Pd^{II} is coordinated with both the double and triple bond is subject to a Jahn−Teller effect[23] and could thus not be located. For the Pd(0) to Pd(II) process, the tricoordinated species **14** leads to **16** through transition structure **15-ts** which has an extraordinarily high Gibbs free energy of activation of 37.2 kcal/mol. The reason is that the d-orbitals of late transition metals are much lower than those of early ones, leading to much smaller d-π^* back-donation, which means neither the acetylene nor the ethylene are effectively activated to give an accessible barrier.[34]

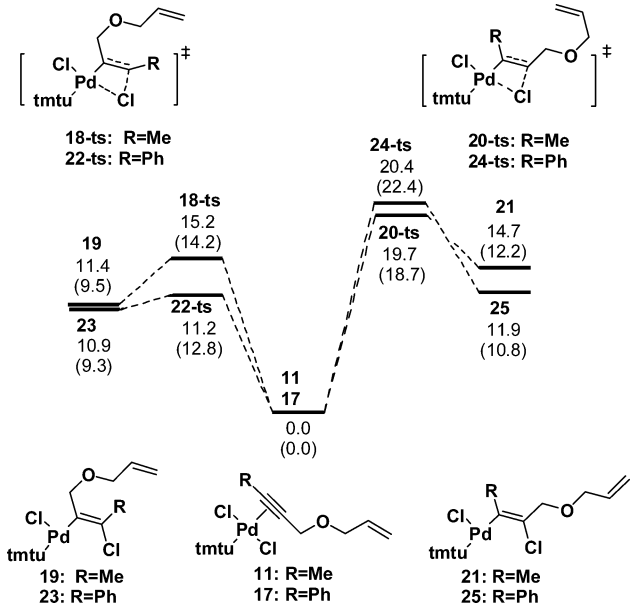

FIGURE 2. Relative Gibbs free energies (in THF) of the two possible initial *cis*-insertion steps with gas phase Gibbs free energies in parentheses.

The C−C coupling reaction of the Pd(II) to Pd(IV) mechanism occurs by the alkene rotating to the top of the Pd-alkyne plane, and then attacking the alkyne through transition structure **12-ts**. The free energy of activation for this step is 30.6 kcal/mol. Compared with the initial step of mechanism B, this mechanism is not reasonable as will be discussed in more detail below.

Halometalation Reaction and Regiochemistry. The alternative mechanism (Pathway B) is initiated by the *cis*-insertion of the Pd−Cl bond to the alkyne. There are two possible regiochemistries for the insertion with either the palladium or the chloride adding to the terminal position of the alkyne. The results for the two possible attacks for the methyl and phenyl substituted substrates **11** and **17**, coordinated to tmtu-$PdCl_2$ are shown in Figure 2.

Both, the Me and Ph substituted, 1,6-enynes show the same preferred regiochemistry for the insertion. The relative Gibbs free energy of activation through **18-ts** is 4.5 kcal/mol lower than **20-ts**, and the relative Gibbs free energy of **22-ts** is 9.2 kcal/mol lower than **24-ts** in THF. The values show that the formation of **19** and **23** is more facile than the formation of the regioisomers **21** and **25**. The insertion is a reversible, endothermic reaction due to the generation of an open coordination site on the palladium. Thus a follow-up reaction, for example the coordination of another ligand such as carbon monoxide or the alkene moiety of the enyne to the vacant site of Pd is necessary to decrease the relative free energy and drive the reaction to completion. The results for these follow-up steps leading to the formation of the final product are shown in Figure 3 for the case of the methyl-substituted reactant. The *cis*- and *trans*- alkyne insertion step was investigated previously by Lu and co-workers.[18a,d,24,25] These results show that when no or only a small quantity (1 equiv or less) of LiCl is added, the *cis*-insertion product is the major stereoisomer formed. Under

(20) Frisch, M. J.; et al. *Gaussian 03*, revision C.02; Gaussian, Inc.: Wallingford, CT, 2004.

(21) (a) Becke, A. D. *J. Chem. Phys.* **1993**, *98*, 1372. (b) Becke, A. D. *J. Chem. Phys.* **1993**, *98*, 5648. (c) Perdew, J. P.; Chevary, J. A.; Vosko, S. H.; Jackson, K. A.; Pederson, M. R.; Singh, D. J.; Fiolhais, C. *Phys. Rev. B* **1993**, *48*, 4978. (d) Perdew, J. P. *Phys. Rev. B* **1986**, *33*, 8822.

(22) (a) Barone, V.; Cossi, M. *J. Phys. Chem. A* **1998**, *102*, 1995. (b) Barone, B.; Cossi, M.; Tomasi, J. *J. Comput. Chem.* **1998**, *19*, 404.

(23) (a) Englman, R. *The Jahn-Teller Effect*; Wiley: New York, 1972. (b) Harvey, P. D.; Reber, C. *Can. J. Chem.* **1999**, *77*, 16.

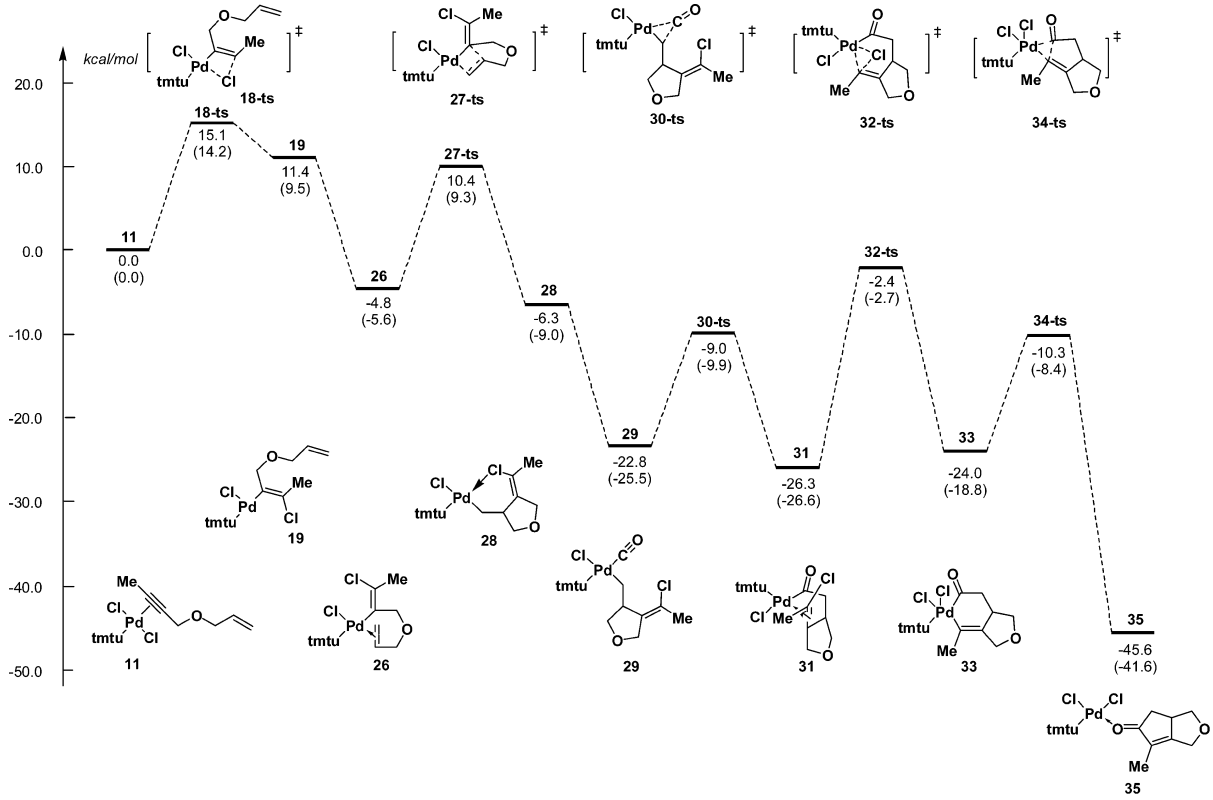

FIGURE 3. Relative Gibbs free energies (in THF) for pathway B steps with gas phase Gibbs free energies in parentheses.

the reaction conditions studied here, the *cis*-alkyne insertion occurs easily due to the preorientation of the Pd−Cl bond. It should be mentioned that the *trans*-insertion may also be possible in the case where more external chloride ions, for example from the lithium chloride addition, are present. Based on the observation that $PdCl_2$ alone is sufficient to catalyze the reaction, this possibility is not further pursued at this point, although the effect of the LiCl amount on the reaction yield will be discussed later.

Pathway B. Figure 3 summarizes the results for the alternative pathway B, which has four major steps. The catalytic cycle begins from the alkyne coordinated intermediate **11**, which is the same initiation step as in the oxidative coupling mechanism, and is set to be the reference energy to provide a direct comparison between the two pathways. After the formation of **19** through the pathway discussed above, the alkene moiety of enyne rapidly occupies the open coordination site to form intermediate **26** in a step that is exergonic by 16.2 kcal/mol. The coordinated alkene is then inserted into the Pd−C bond via the transition structure **27-ts** with a barrier of 15.2 kcal/mol. The alkene insertion product **28** has formally an open coordination site, but is 1.5 kcal/mol more stable than intermediate **26**. This suggests an additional stabilization by intramolecular coordination to the vinyl chloride, which in turn is rapidly displaced by carbon monoxide to form intermediate **29** with a 16.5 kcal/mol Gibbs free energy decrease. It should be pointed out that this exergonicity is overestimated by ∼2−3 kcal/mol because the loss of entropy from translational and rotational degrees of freedom in the bimolecular reaction are not considered in the calculations. The first of the two carbon−carbon bond formation where the coordinated carbon monoxide inserts into the Pd−C bond occurs via transition structure **30-ts**. The barrier of the carbon monoxide insertion is about 13.8 kcal/mol, being relatively low. The stable alkene coordinated intermediate **31** is formed with 3.5 kcal/mol Gibbs free energy decrease.

The key step of the new mechanism proposed here is the oxidative addition of the palladium into the vinylic carbon-chloride bond via transition structure **32-ts**, forming the Pd^{IV} intermediate **33**. Although the Pd^{II} to Pd^{IV} transformation with oxidative additions to carbon-bromide or carbon-iodide has been described in both experimental[26] and computational studies,[27] there is to the best of our knowledge little precedence for the addition into a carbon-chloride bond in the literature. This step will therefore be discussed in more detail later. Nevertheless, the results clearly indicate that the Gibbs free energy of activation of this step is with 23.9 kcal/mol in THF (23.9 kcal in the gas phase) almost 7 kcal/mol lower than the rate determining step (via **12-ts**) of the oxidative coupling mechanism, which was calculated to be 30.6 kcal/mol at the same level of theory. The product of this reaction, the palladium-containing six-member ring **33** is formed with a 2.3 kcal/mol increase in Gibbs free energy. The reductive elimination via **34-ts** has a barrier of only 13.7 kcal/mol, leading to the

(24) (a) Ma, S.; Lu, X. *J. Org. Chem.* **1991**, *56*, 5120. (b) Ma, S.; Zhu, G.; Lu, X. *J. Org. Chem.* **1993**, *58*, 3692.

(25) (a) Wang, Z.; Zhang, Z.; Lu, X. *Organometallics* **2000**, *19*, 775. (b) Zhang, Z.; Lu, X.; Xu, Z.; Zhang, Q.; Han, X. *Organometallics* **2001**, *20*, 3724.

(26) (a) Canty, A. J. *Acc. Chem. Res.* **1992**, *25*, 83, and references cited therein. For a recent X-ray structure of a Pd(IV) species, see: (b) Guo, R. Y.; Portscheller, J. L.; Day, V. W.; Malinakova, H. C. *Organometallics* **2007**, *26*, 3874. (c) Bressy, C.; Alberico, D.; Lautens, M. *J. Am. Chem. Soc.* **2005**, *127*, 13148. (d) Faccini, F.; Motti, E.; Catellani, M. *J. Am. Chem. Soc.* **2004**, *126*, 78. (e) Whitfield, S. R.; Sanford, M. S. *J. Am. Chem. Soc.* **2007**, *129*, 15412. (f) Furuya, T.; Ritter, T. *J. Am. Chem. Soc.* **2008**, *120*, 10060.

(27) Sundermann, A.; Uzan, O.; Martin, J. M. L. *Chem.—Eur. J.* **2001**, *7*, 1703.

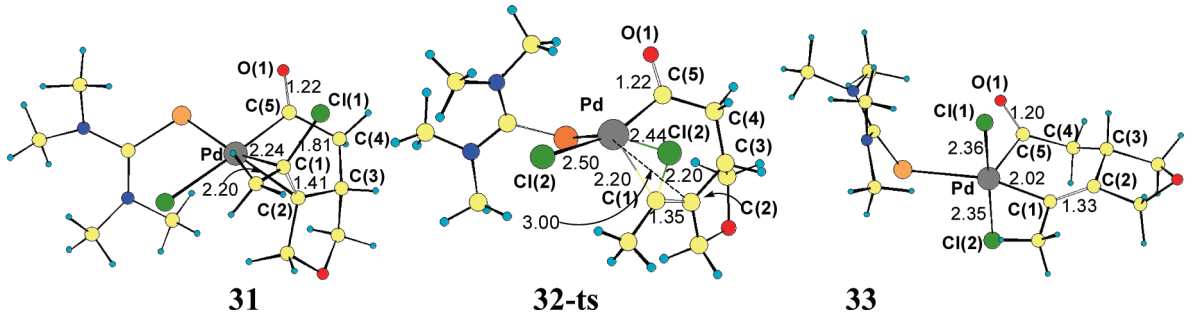

FIGURE 4. Calculated geometries of key intermediates and transition structures of the two proposed pathways. Bond lengths are in Å.

cyclopentenone coordinated to Pd^{II} complex **35**. This rapid follow-up reaction is exergonic by 21.6 kcal/mol, rendering the overall reaction effectively irreversible. As will be discussed in more detail below, this pathway is not only energetically more favorable, but also in better agreement with the other experimental findings.

The calculated geometries of intermediates **31** and **33** as well as the rate-determining transition structure **32-ts** are shown in Figure 4. In **31**, the alkene coordination discussed above is reflected in the short bond lengths of the Pd−C(1) bond and Pd−C(2) bond if 2.24 Å and 2.20 Å, respectively. The carbon−carbon bond length of the olefin is 1.41 Å, much longer than a typical C=C double bond. This observation can be rationalized by a combination of donation of π-electrons from the olefin to the coordinated Pd^{II} and the back-donatation from the d-orbitals of Pd^{II} to the antibonding π^* orbital. Both effects lead to the increase of C=C bond length. In contrast, the bond length of C(1)−Cl(1) is 1.81 Å, close to a normal carbon-chloride single bond. In **32-ts**, Cl(1) is with a distance of 2.44 Å coordinated but not completely bonded to the palladium, as can be seen by comparison with the Pd−Cl bond of 2.35 Å in **33**. The C(1)−Cl(1) bond is weakened by this coordination to a bond length of 2.20 Å, much longer than the same bond in **31**. C(2) is completely dissociated from the metal, the distance between Pd and C(2) is 3.00 Å. The structure of **32-ts** shows that the coordination of alkene is weakened and the C(1)−Cl(1) bond is broken, but the Pd−Cl(1) and Pd−C(1) bonds have not been fully formed yet. Consistent with that, the energy of **32-ts** is relatively high. The key intermediate **33** is then formed via oxidative addition. The palladium adopts the characteristic square pyramidal coordination geometry described previously for Pd^{IV},[27] although the vacant site of the octahedron could also be occupied by a THF solvent molecule to complete the coordination sphere.

CO Insertion and Olefin Insertion Sequence. A key feature of our proposed mechanism is the order in which insertions occur. After the alkyne inserted into the Pd−C(l) bond, carbon monoxide insertion is a competitive reaction. Figure 5 compares the Gibbs free energies for the alkene and the carbon monoxide insertions. Although carbon monoxide is in most cases a better ligand than an alkene, in the case of an intra- vs. intermolecular coordination, the relative free energy of carbon monoxide coordinated intermediate **36** and the alkene coordinated intermediate **26** are nearly the same because of the entropy loss when carbon monoxide coordinated to Pd. The barrier for carbon monoxide insertion via transition structure **37-ts** is only about 9.3 kcal/mol, but the insertion product **38** is only 2.8 kcal/mol more stable than **36**. In comparison, the product of the alkene coordination to palladium, intermediate **39**, is 3.6 kcal/mol more stable than **38**. Thus, it can be expected that intermediates **26**, **36**, **38** and **39** will be in rapid equilibrium. When intermediate **39** is formed, the alkene is likely to insert into the Pd−C bond. However, the barrier of the alkene insertion step is 29.8 kcal/mol. The Gibbs free energy of the transition structure **40-ts** is 9.9 and 14.1 kcal/mol higher than **27-ts** and **37-ts**, respectively. Therefore, it is unlikely that **41** can be formed through this pathway and **39** will reverse to **26**, and further react to **29**. The barrier of complete pathway from **39** to **29** is only 20.9 kcal/mol, compared to a barrier for the reaction of **39** to **41** of 29.8 kcal/mol.

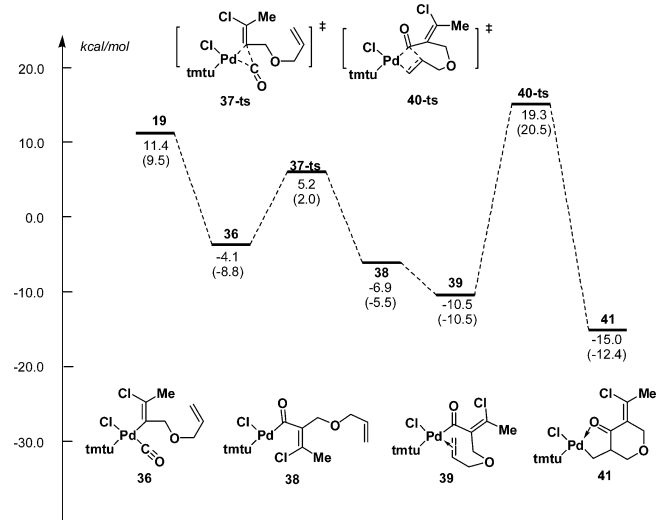

FIGURE 5. Relative Gibbs free energies (in THF) of the competitive carbonyl insertion reaction with gas phase Gibbs free energies in parentheses.

Generation of the Pd(IV) Intermediate. The rate determining key step of pathway B is the oxidative addition to form a Pd^{IV} species. Although there is some precedence for the formation of Pd^{IV} through oxidative addition to carbon-iodide and carbon-bromide bonds,[26,27] some of this work is controversial[35] and may only apply to the sp^3 carbons studies there. In comparison, there are only few, intramolecular examples for the addition to crbon-chloride bonds.[36] This limited precedence prompted an investigation of the different effects that might be able to stabilize the Pd^{IV}.

We started our investigation by considering the inter- vs. intramolecular reaction, shown in Figure 6. The intramolecular binding of olefin leads to about 10.5 kcal/mol enthalpy release in THF (from **31a** to **31**). Taking the entropy loss into account, the relative free energy of **31** is about 5.3 kcal/mol lower than **31a** in THF. Thus, the overall activation free energy for the formation of Pd(IV) intermediate **33** is about 24.0 kcal/mol (from **31** to **32-ts**). The intermediate **33** is only about 2.3 kcal/mol endogonic relative to **31** in terms of free energy. A similar

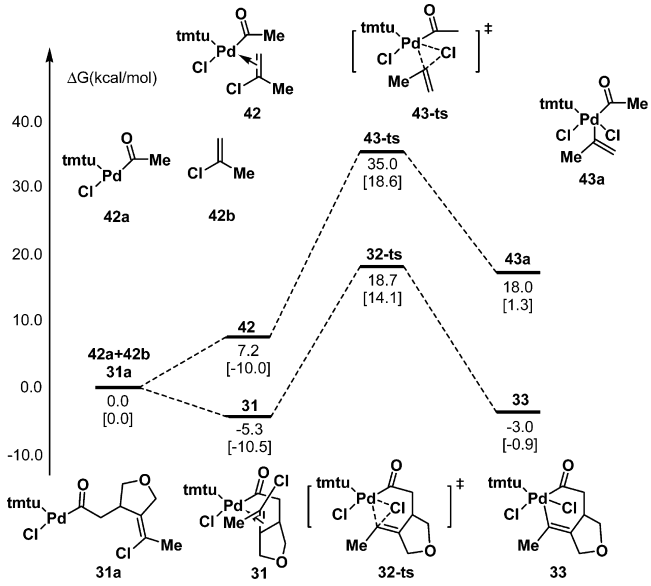

FIGURE 6. Comparison of Gibbs free energies (in THF) for the inter- and intramolecular oxidative addition with enthalpy values (in THF) in parentheses.

model of **42a** and 2-chloride propene **42b** are used to study the corresponding intermolecular oxidative addition. The binding enthalpy of **42b** is about 10.0 kcal/mol in THF, just the same as the intramolecular result. Yet the entropy loss causes **42** to be about 7.2 kcal/mol higher than **42a** and **42b** in terms of free energy in THF. The activation free energy of the oxidative addition for intermolecular C−Cl bond is 27.8 kcal/mol in THF (from **42** to **43-ts**). Thus, the overall barrier for the formation of Pd(IV) intermediate **43a** is 35.0 kcal/mol (from **42a**+**42b** to **43-ts**). And the intermediate **43a** is about 18.0 kcal/mol endogonic (from **42a**+**42b** to **43a**). Thus the generation of intermolecular oxidative addition Pd(IV) intermediate **43a** is not only kinetically, but also thermodynamically unfavorable.

To probe the electronic influence of the ligands coordinated to the palladium, we studied additional model systems for the

TABLE 1. Free Energy Barriers for the Oxidative Addition in Different Model Systems

Entry	substrate	transition state	barrier (kcal/mol)
1	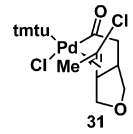 31	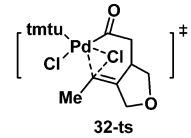 32-ts	24.0
2	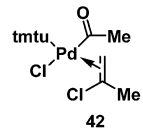 42	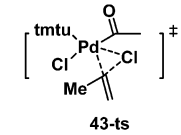 43-ts	27.8
3	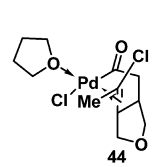 44	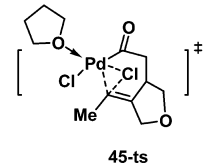 45-ts	27.6
4	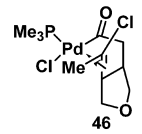 46	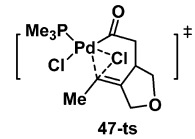 47-ts	24.0
5	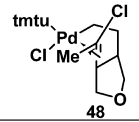 48	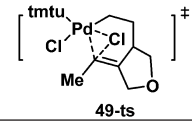 49-ts	21.2

SCHEME 3. Experimentally Observed Diastereoselectivities[12]

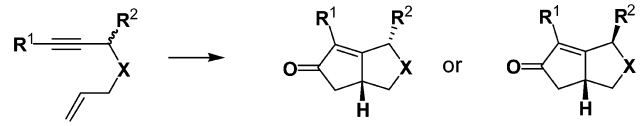

	catalyst				total yield
a: X=NTs, R^1=4-$C_6H_4NO_2$ R^2= n-C_5H_{11}	$PdCl_2$, TMTU	1	:	0	96 %
b: X=O, R^1=C_6H_5 R^2= CH_3	$PdCl_2$, TMTU	9	:	1	70 %
	$CpTi(CO)_2$	1	:	10	94 %

oxidative addition. As can be seen from the results summarized in Table 1, replacement of the tmtu ligand with a THF solvent increases the barrier for the intramolecular oxidative addition to 27.6 kcal/mol (entry 3), close to the value for the intermolecular reaction. This is in agreement with the experimental finding that the tmtu ligand increases the reaction rate.[12] A similar stabilization can be achieved using the electron rich PMe_3 ligand (entry 4). Conversely, replacement of the electron withdrawing acyl group by a methylene lowers the free energy of activation to 21.2 kcal/mol (entry 5). These findings are consistent with the idea that a polarizable, Lewis-basic ligand stabilizes the transition state for the formation of the Pd^{IV} intermediate whereas electron withdrawing groups or less Lewis basic ligands increase the barrier for the formation of the high oxidation state of the palladium. The stabilization by tmtu is also the reason why the novel mechanism involving the Pd^{IV} intermediate is energetically more favorable than the traditional

(28) There are no directly comparable examples of 3-methyl-1,6-enyne in Co catalyzed PKR, but 3-TBSO-1,6-enyne in the references below show the stereochemistry of Co catalyzed PKR. (a) Krafft, M. E.; Bonaga, L. V. R.; Hirosawa, C. *Tetrahedron Lett.* **1999**, *40*, 9171, Entry 12 and 13. (b) Breczinski, P. M.; Stumpf, A.; Hope, H.; Krafft, M. E.; Casalnuovo, J. A.; Schore, N. E. *Tetrahedron* **1999**, *55*, 6797, Table 2. (c) Moriarty, R. M.; Rani, N.; Enache, L. A.; Rao, M. S.; Batra, H.; Guo, L.; Penmasta, R. A.; Staszewski, J. P.; Tuladhar, S. M.; Prakash, O.; Crich, D.; Hirtopeanu, A.; Gilardi, R. *J. Org. Chem.* **2004**, *66*, 1890.

(29) A direct comparison for **42**c is not possible because this substrate undergoes a series of side reactions leading to undefined product mixtures.

(30) (a) Tietze, L. F.; Schulz, G. *Liebigs Ann.* **1996**, 1575. Compare also: (b) Allinger, N. L.; Hirsch, J. A.; Miller, M. A.; Tyminski, J. *J. Am. Chem. Soc.* **1968**, *90*, 5773.

(31) (a) Neumann, F.; Hampel, F.; Schleyer, P. V. *Inorg. Chem.* **1995**, *34*, 6553. (b) Jiao, H. J.; Schleyer, P. V. *J. Am. Chem. Soc.* **1995**, *117*, 11529.

(32) (a) Holzapfel, C. W.; Marais, L. *Tetrahedron Lett.* **1997**, *38*, 8585. (b) Lu, X. *Top. Catal.* **2005**, *35*, 73. (c) Wang, Z.; Zhang, Z.; Lu, X. *Organometallics* **2000**, *19*, 775. (d) Wang, Z.; Lu, X. *Tetrahedron Lett.* **1997**, *38*, 5213. (e) Zhang, Z.; Lu, X.; Xu, Z.; Zhang, Q.; Han, X. *Organometallic* **2001**, *20*, 3724.

(33) Bäckvall, J. E.; Nilsson, Y. I. M.; Gatti, R. G. P. *Organometallics* **1995**, *14*, 4242.

(34) Imabayashi, T.; Fujiwara, Y.; Nakao, Y.; Sato, H.; Sakaki, S. *Organometallics* **2005**, *24*, 2129.

(35) (a) Consorti, C. S.; Flores, F. R.; Dupont, J. *J. Am. Chem. Soc.* **2005**, *127*, 12054. (b) Bergbreiter, D. E.; Osburn, P. L.; Frels, J. D. *Adv. Synth. Cat.* **2005**, *347*, 172.

(36) Liebeskind, L. S.; Baysdon, S. L.; South, M. S.; Iyer, S.; Leeds, J. P. *Tetrahedron* **1985**, *41*, 5839.

(37) For example: (a) Tanaka, K.; Fu, G. C. *J. Am. Chem. Soc.* **2001**, *123*, 11492. (b) Onitsuka, K.; Segawa, M.; Takahashi, S. *Organometallics* **1998**, *17*, 4335.

SCHEME 4. Transition States for the Formation of the Diastereomeric Products 51 and 52

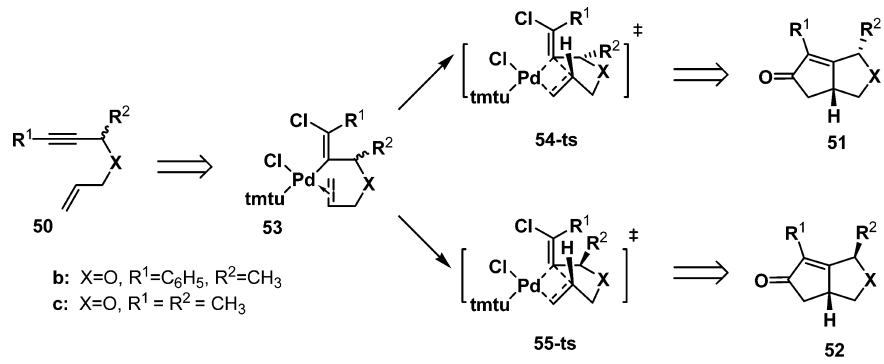

Magnus mechanism, which is energetically prohibitive in the case of late transition metals such as palladium.

Diastereoselectivity of the Reaction. As mentioned earlier, the new mechanism presented here is not only found to be energetically more favorable for the palladium catalyzed PKR, but is also in better agreement with the experimental observations. As shown in Scheme 3, we found that the diastereoselectivity of allylic alkane substituted 1,6-enyne is opposite to the one described obtained with other transition metal catalysts.[5b,28] If the racemic substrates **50a,b** are used in the palladium catalyzed PRK, the major products are **51** as is unambiguously demonstrated by the X-ray structure of product **51b** (See Supporting Information). In contrast, the $TiCp_2$[5b] and $Co_2(CO)_8$[28] catalyzed PKR give the products **52** as the major products. Similar results were obtained for diyne **50b**, which gave under Pd catalyzed PKR condition the product **51b** as the major product with a d:r of 9:1.

The diastereoselectivity of the reaction is determined by the position of the alkene moiety of the enyne in the insertion step. As shown in Figure 3, this step is irreversible and sets the stereochemistry based on the relative energies of the diastereomeric transition states. For the substrates shown in Scheme 4, **50b** and **50c**, there are two possible alkene insertion transition structures for the formation of the diastereomers from the complex **53**. The product **51**, in which the bridgehead hydrogen and the substituents R^2 are *trans* to each other, is produced via **54-ts**, and product **52** with the corresponding *cis* stereochemistry is produced via **55-ts**. We have calculated the relative energies of the different possible transition structures **54-ts** and **55-ts** for the two model substrates **50b** and **50c** to elucidate the origin of the experimentally observed stereochemistry in the Pd catalyzed PKR. The results are summarized in Figure 7.

It can be seen that the relative energies of **54-ts** and **54c-ts**, leading to the experimentally observed products, are significantly lower than that for the diastereomeric transition structures **55b-ts** and **55ts**. In both cases, the transition structures **55** are subject to a significant 1,3-allylic strain due to the *cis*- arrangement of the substituents R_1 and R_2 in the allyl system. This repulsive interaction favors the *trans* arrangement of the substituents in **55b-ts** and **55c-ts** by 3.2 and 3.0 kcal/mol, respectively. Although the energy differences are overestimated as compared to the experimentally observed selectivities of approximately 9:1 for **50b**,[29] they are consistent with other computational studies of 1,3-allyl strain.[30] This overestimation is common in such studies where only a single conformer is considered because the reaction will also proceed through other, slightly higher energy transition state conformations not considered here. More importantly, these results rationalize the experimentally observed diastereoselectivity based on the stereoselecting transition structures of the novel mechanism and allow the semiquantitative prediction of the diastereomer formed.

Effect of LiCl. Based on the earlier observation that chloride is necessary for the reaction to occur and the computational results discussed above, we reinvestigated the reaction and found that the presence of LiCl speeds up the reaction and ultimately increases the isolated yield. Interestingly, neither LiBr nor NaCl show similar enhancements.[12b] We therefore calculated a model system of the palladium catalyzed PKR containing LiCl. The resulting energy profile is shown in Figure 8. In solution, LiCl will be solvated by THF,[31] leading to a tetrahedral lithium complex modeled here by $LiCl(Me_2O)_3$. $LiCl(Me_2O)_3$ is bonding to **31** and dissociates two Me_2O molecules to form intermediate **56**. The calculated free energy change of this step is 7.8 kcal/mol. While this value might not be accurate due to increased charge delocalization in the small model system, it is clear that **31** and **56** will be in equilibrium favoring the later. Coordination of the lithium species stabilizes transition structure **57-ts** and the activation free energy from **56** to **57-ts** is reduced to 22.0 kcal/mol. For comparison, the free energy of activation from **31** to **32-ts** is 23.9 kcal/mol, consistent with the experimentally observed rate increase. The overall reaction energy to form intermediate **58** via **57-ts** is also 7.6 kcal/mol less endergonic than in the case of **33**. This is in agreement with the earlier observation that the yield increases from only a trace amount

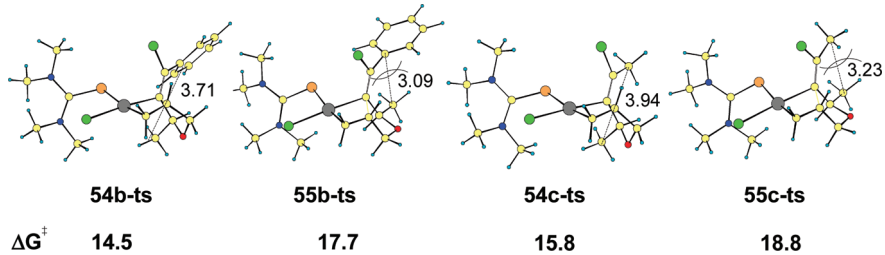

FIGURE 7. Geometries and free energies of activation of stereoselecting transition structures in pathway B.

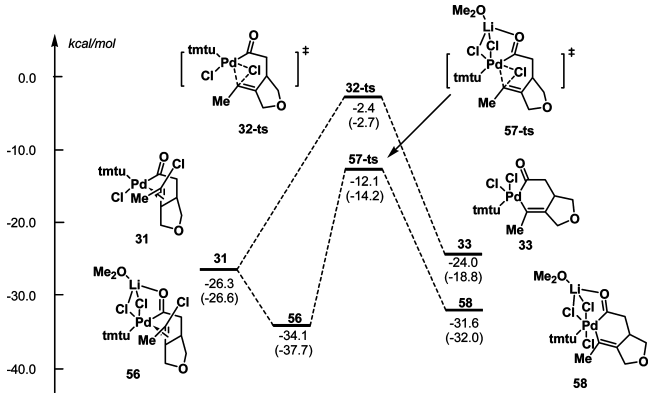

FIGURE 8. Relative Gibbs free energies (in THF) of the oxidative addition step in the presence of LiCl with gas phase Gibbs free energies in parentheses.

of the product present to 82%, using only 1 mol % of LiCl as a cocatalyst.[12b]

The origin of these changes in the relative free energies can be rationalized by analysis of the geometries of **56**, **57-ts** and **58**, shown in Figure 9. For all structures, it appears that one reason for the stabilization is that the chloride coordinates to the open site on the palladium in the different species along the reaction pathway while the lithium coordinates in a chelate fashion to two chlorides and the carbonyl oxygen. The bond lengths of Pd−C(1) and Pd−C(2) in **56** are 2.16 Å and 2.17 Å, much shorter than the same bonds in **31**. Conversely, the bond length of C(1)−C(2) in **56** is 1.43 Å, longer than the same bond in **31**. This is consistent with a stronger coordination of palladium to the olefin up to the point were the Pd−C(1) and Pd−C(2) bonds have some single bond character. In this coordination sphere, the palladium with be electronically closer to a +IV oxidation state character that is stabilized by the chloride as well as by a stronger coordination of the olefin. A d-π* back-donation into the double bond would also decrease the electron density of palladium, leading to a stronger coordination of the vinylic chloride. In agreement with this interpretation, the distance between Pd and Cl(3) in **56** is 2.63 Å. Though longer than a typical Pd−Cl single bond, it clearly shows a strong interaction. The distance between Pd and Cl3 in **57-ts** is decreased to 2.58 Å and the Li−Cl(3) distance is increased to 2.35 Å, indicating that the interaction Pd−Cl(3) interaction increases as the Pd−C(2) interaction decreases. In this approximately octrahedral geometry in **57-ts**, the forming Pd−C(1) bond length is 2.18 Å with Cl(3) occupying the trans-position relative to the forming bond. The coordination in intermediate **58** is also octahedral. Because of the strong *trans*-effect, the bond length of Pd−Cl(3) is significantly longer than the ones of Pd−Cl(1) and Pd−Cl(2). The octahedral environment is further stabilized by the chelation by the lithium which would be much weaker in the case of sodium or potassium.

Trans Halometalation of Alkyne. Although the novel mechanism presented here is consistent with the experimental observations, alternatives to the oxidative addition step need to be considered. Specifically, a direct *trans*-halometalation of the alkyne followed by an insertion of the vinyl chloride moiety into the acylpalladium species and chloride elimination could rationalize the formation of **35** without the involvement of the Pd^{IV} species. Previously, the *trans*-insertion was found to be competitive to the *cis*-insertion when large concentrations of LiCl, which could presumably facilitate the *trans*-halometalation by attack of the chloride trans to the palladium, are used.[32] Insertions of haloalkenes in acyl-palladium intermediates have also been reported.[37] We therefore decided to investigate this alternative mechanism.

The Gibbs free energy surface for this alternative mechanism is shown in Figure 10. We were unable to locate the transition structure of the *trans*-alkyne insertion, but the insertion intermediate **59** is found to be more stable than *cis*-insertion intermediate **26**. Furthermore, all intermediates and transition structures of *trans*-insertion mechanism (**59**−**64**) are 1−2 kcal/mol more stable than the corresponding structures in the case of the *cis*-insertion mechanism (**26**−**31**). After insertion of the olefin and the carbonyl, the fairly stable intermediate **64** is formed. However, the key insertion step via **65-ts** has a very large free energy of activation of 38.5 kcal/mol, rendering this step prohibitive. Therefore, if the *trans*-insertion were to take place, it would lead to the stable intermediates **62** and **64** that cannot react further.

The geometry of transition structure **65-ts**, shown in Figure 11, provides some insight into the high barrier of this step. Comparison with the alternative transition structure **32-ts** reveals significant strain is present in the [2.1.1] bicyclic system formed by Pd, C(2), C(1) and C(5) and the five-membered ring. This leads for example to a compression of the C(2)−C(1)−C(5) angle to 53° and to several eclipsed interactions that are not present in **32-ts**.

The results shown in Figure 10 are also consistent with the fact that, because they are easily formed but a further reaction via transition structures such as **65-ts** is energetically prohibitive, the products of the *trans*-insertion can be trapped in certain cases.[33] In the present example, **62** or **64** cannot revert to the starting materials based on the overall exergonicity of the reaction. It is most likely that these intermediates will decompose, thus lowering the overall yield of the reaction. To test

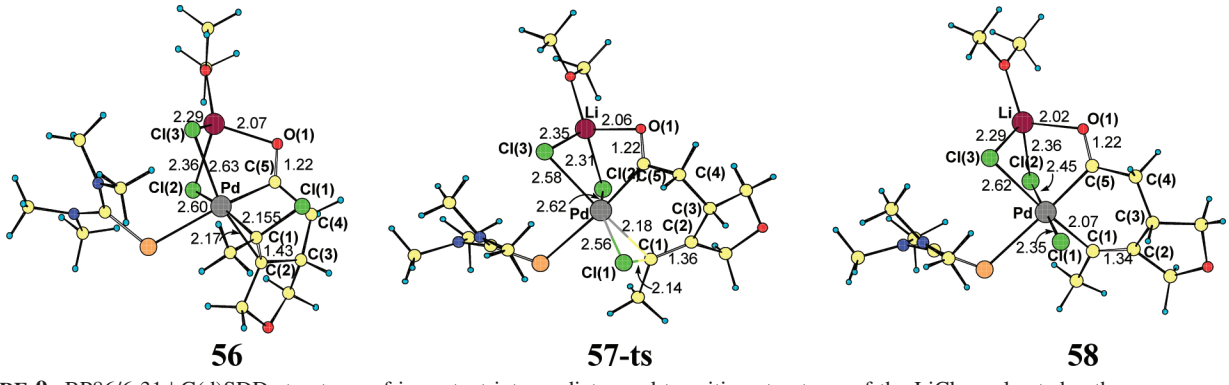

FIGURE 9. BP86/6-31+G(d)SDD structures of important intermediates and transition structures of the LiCl-accelerated pathway.

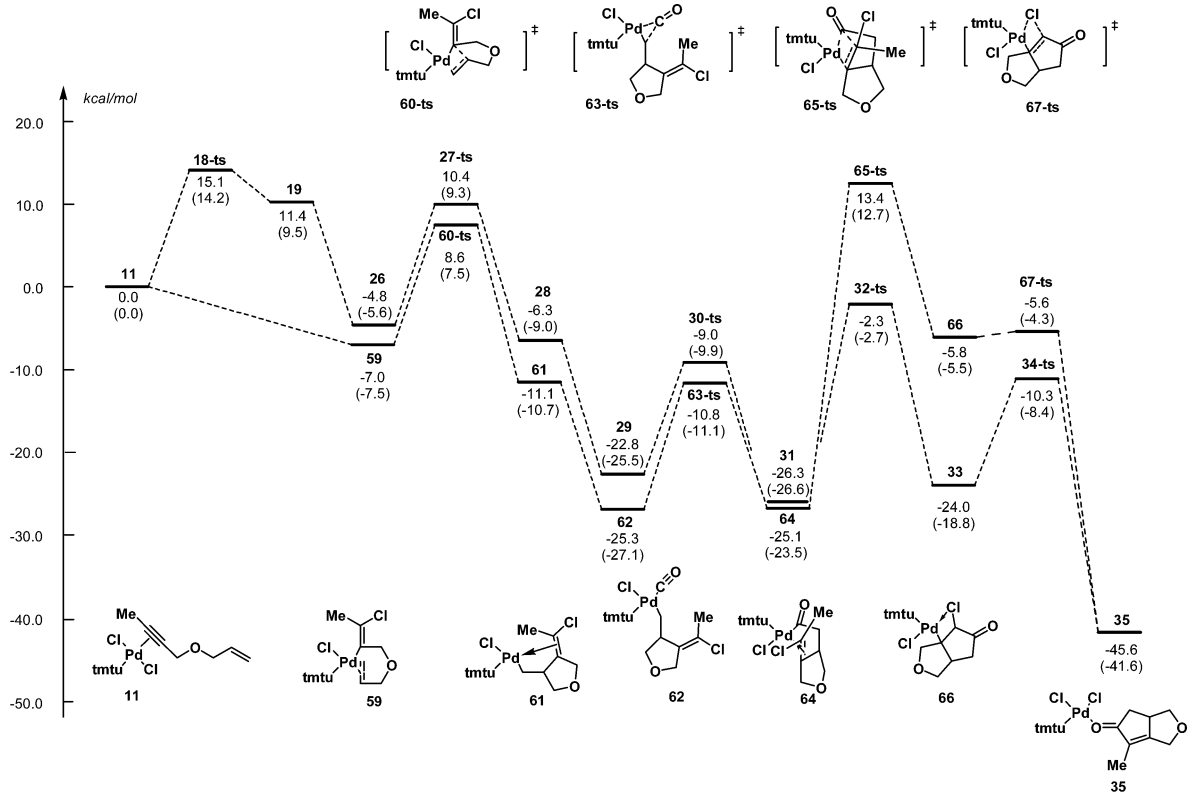

FIGURE 10. Relative Gibbs free energies (in THF) for the alternative *trans*- alkyne insertion mechanism with gas phase Gibbs free energies in parentheses.

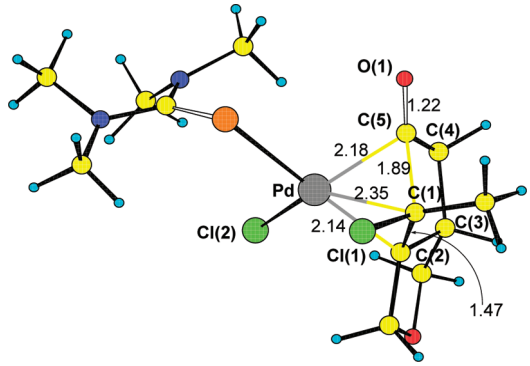

FIGURE 11. Structure of **65-ts**.

TABLE 2. Dependence of Product Yield on the Amount of LiCl

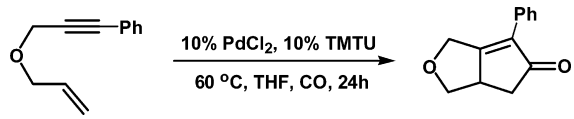

equivalent of LiCl	yield of product
0.5	29%
1.0	36%
2.0	42%
5.0	25%
10.0	22%

this hypothesis, we studied the effect of the amount of LiCl on the reaction yield and the results are summarized in Table 2. When 2 eq of LiCl were used in the reaction, the *cis*- insertion is the major pathway and the usual product is formed. An increase of the amount of LiCl to 5 or more equivalents would lead, in agreement with previous experimental results,[33] to an increased *trans*-insertion and ultimately to a decreased product yield. Unfortunately, we were unable to isolate other products in this case and no remaining starting material was observed.

Conclusions

In conclusion, we present a novel mechanism for the palladium catalyzed Pauson−Khand-type reaction that involves an oxidative addition to a C−Cl bond resulting in the formation of a Pd^{IV} species, which has to the best of our knowledge not been previously described. The free energies of activation for this pathway were calculated to be ∼4 kcal/mol more favorable than the ones for the classical Magnus mechanism initiated by oxidative coupling of the olefin. An alternative mechanism involving a *trans*-hydrometalation was also found to be energetically prohibitive. More importantly, the new mechanism accounts for a series of experimental observations that would be hard to explain in the classical mechanism. Specifically, the effect of Cl^- can be explained by the necessity of a *cis*-addition to the alkyne for the following key oxidative addition into the vinyl chlorine bond, which also rationalizes the previous observations by Bäckvall et al.[33] The observed diastereoselectivity, which is opposite from other PKRs and therefore synthetically useful, can be explained by the a 1,3-allylic strain, leading to a repulsive interaction of the substituents in the α-position and the terminal position of the alkyne in the stereoselecting transition structures. Finally, the effect of experimentally observed rate acceleration by LiCl addition can be rationalized by stabilization of the Pd^{IV} obtained in the oxidative addition step by a coordinated chloride and the stabilization of the octahedral coordination[26b] of the Pd^{IV} species by a chelating lithium. Further increase of the amount of LiCl was found to decrease

the product yield, presumably by favoring the *trans*-insertion that does not lead to product formation.

Further studies of the scope and limitations of the novel oxidative addition step as well as the LiCl catalysis of metalorganic reactions, for which the detailed knowledge of the geometric and electronic structure of the transition structures and intermediates involved in the Pd-catalyzed PRK should be useful in expanding the application of this synthetically useful reaction. Specifically, the dependence of the stability of the Pd^{IV} intermediate, which has found significant interest in the recent literature,[26] should also be transferable to other cases. The unique role of the thiourea ligand, which was previously postulated to stabilize the high oxidation state of the palladium in a carbon monoxide environment,[12] could lead to the development of an enantioselective version of this reaction. This and additional studies of intermolecular examples of the reaction are currently in progress and will be reported in upcoming publications.

Experimental Section

Flash chromatographic separations were carried out on Silica gel (200−300 mesh).^{1}H NMR and ^{13}C NMR were recorded on a 300 MHz spectrometer or a 400 MHz spectrometer. $LiCl \cdot H_2O$ was flame-dried before being evacuated by oil pump, and was stored in desiccators. All the weighing manipulations were conducted under aerobic conditions. THF was distilled from sodium under nitrogen atmosphere. **50b** was prepared following literature methods.[12a,38]

(38) (a) Kobayashi, T.; Koga, Y.; Narasaka, K. *J. Organomet. Chem.* **2001**, *624*, 73. (b) Krafft, M. E.; Romreo, R. H.; Scott, I. L. *J. Org. Chem.* **1992**, *57*, 5277.

Compound 51b and 52b.

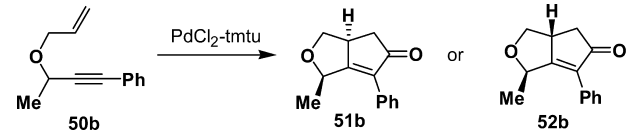

Typical Procedure for the Compound 51b and 52b. Procedure A: To a mixture of $PdCl_2$ (8.9 mg, 0.05 mmol), TMTU (6.6 mg, 0.05 mmol) and LiCl (21 mg, 0.5 mmol) in dry THF charged with CO balloon was added **50b** (93 mg, 0.5 mmol) in 15 mL THF. The reaction mixture was stirred at 60 °C for 48 h. Then, the solvent was removed under reduced pressure, and the residue was purified by flash chromatograph (petrol ether/ethyl acetate = 6:1), to afford **51b** and **52b** (75 mg, 70%) as colorless oil. Procedure B: To a mixture of $PdCl_2$ (8.9 mg, 0.05 mmol) and TMTU (6.6 mg, 0.05 mmol) in dry THF charged with CO balloon was added **50b** (93 mg, 0.5 mmol) in 15 mL THF. The reaction mixture was stirred at 60 °C for 48 h. Then, the solvent was removed under reduced pressure, and the residue was purified by flash chromatograph (petrol ether/ethyl acetate = 6:1), to afford **51b** and **52b** (48 mg, 45%) as colorless oil.

Spectroscopic Data for 52b. ^{1}H NMR (200 MHz, $CDCl_3$): 1.15 (d, J = 6.4 Hz, 3 H), 2.35 (dd, J = 3 Hz, J = 17.8 Hz, 1 H), 2.81 (dd, J = 5.4 Hz, J = 18.2 Hz, 1 H), 3.36−3.39 (m, 2 H),4.29−4.30 (m, 1 H), 5.23 (q, J = 6.4 Hz, 1H), 7.26−7.40 (m, 5H); ^{13}C NMR (50 MHz, $CDCl_3$): δ 17.2, 40.0, 45.0, 69.4, 72.8, 128.3, 128.4, 129.0, 130.0, 154.9, 182.1, 207.1; LRMS (EI): 214 (M^+).

Acknowledgment. We are grateful to the National Natural Science Foundation of China (20225312, 20325208, and 20832003) and the Research Grants Council of Hong Kong for financial support of the research.

Supporting Information Available: Cartesian coordinates of all structures discussed, computational details as well as X-ray structure determination of **51b**. This material is available free of charge via the Internet at http://pubs.acs.org.

JO900919V